HHS Public Access

Author manuscript

Basic Res Cardiol. Author manuscript; available in PMC 2018 May 01.

Published in final edited form as:

Basic Res Cardiol. 2017 May ; 112(3): 23. doi:10.1007/s00395-017-0612-7.

Cardiomyocyte *Ogt* limits ventricular dysfunction in mice following pressure overload without affecting hypertrophy

Sujith Dassanayaka[1], **Robert E. Brainard**[1], **Lewis J. Watson**[1,2], **Bethany W. Long**[1], **Kenneth R. Brittian**[1], **Angelica M. DeMartino**[1], **Allison L. Aird**[1], **Anna M. Gumpert**[1], **Timothy N. Audam**[1], **Peter J. Kilfoil**[1], **Senthilkumar Muthusamy**[1], **Tariq Hamid**[1,3], **Sumanth D. Prabhu**[1,3], and **Steven P. Jones**[1]

[1]Division of Cardiovascular Medicine, Department of Medicine, Institute of Molecular Cardiology, Diabetes and Obesity Center, University of Louisville, 580 South Preston Street, Louisville, KY 40202, USA

Abstract

The myocardial response to pressure overload involves coordination of multiple transcriptional, post-transcriptional, and metabolic cues. The previous studies show that one such metabolic cue, O-GlcNAc, is elevated in the pressure-overloaded heart, and the increase in O-GlcNAcylation is required for cardiomyocyte hypertrophy in vitro. Yet, it is not clear whether and how O-GlcNAcylation participates in the hypertrophic response in vivo. Here, we addressed this question using patient samples and a preclinical model of heart failure. Protein O-GlcNAcylation levels were increased in myocardial tissue from heart failure patients compared with normal patients. To test the role of OGT in the heart, we subjected cardiomyocyte-specific, inducibly deficient *Ogt* (i-cm*Ogt*$^{-/-}$) mice and *Ogt* competent littermate wild-type (WT) mice to transverse aortic constriction. Deletion of cardiomyocyte *Ogt* significantly decreased O-GlcNAcylation and exacerbated ventricular dysfunction, without producing widespread changes in metabolic transcripts. Although some changes in hypertrophic and fibrotic signaling were noted, there were no histological differences in hypertrophy or fibrosis. We next determined whether significant differences were present in i-cm*Ogt*$^{-/-}$ cardiomyocytes from surgically naïve mice. Interestingly, markers of cardiomyocyte dedifferentiation were elevated in *Ogt*-deficient cardiomyocytes.

Correspondence to: Steven P. Jones.

[2]Present Address: Kentucky College of Osteopathic Medicine, University of Pikeville, Pikeville, KY, USA

[3]Present Address: Division of Cardiovascular Disease and Comprehensive Cardiovascular Center, University of Alabama at Birmingham, Birmingham, AL, USA

S. Dassanayaka and R. E. Brainard contributed equally to this work.

Electronic supplementary material The online version of this article (doi: 10.1007/s00395-017-0612-7) contains supplementary material, which is available to authorized users.

Compliance with ethical standards

Conflict of interest

None.

Author contributions SD performed experiments, analyzed data, generated figures, wrote draft, revised manuscript, and provided funding. REB performed experiments, analyzed data, generated figures, and wrote draft. LJW performed experiments and analyzed data. BWL performed experiments and analyzed data. KRB performed experiments and analyzed data. AMM performed experiments, generated figures, and analyzed data. AMA performed experiments and analyzed data. AMG performed experiments and analyzed data. TNA performed experiments and analyzed data. PJK performed experiments and revised manuscript. SM performed experiments and analyzed data. TH performed experiments and analyzed data. SDP designed experiments, revised manuscript, and provided funding. SPJ designed experiments, wrote draft, revised manuscript, and provided funding.

Although no significant differences in cardiac dysfunction were apparent after recombination, it is possible that such changes in dedifferentiation markers could reflect a larger phenotypic shift within the *Ogt*-deficient cardiomyocytes. We conclude that cardiomyocyte *Ogt* is not required for cardiomyocyte hypertrophy in vivo; however, loss of *Ogt* may exert subtle phenotypic differences in cardiomyocytes that sensitize the heart to pressure overload-induced ventricular dysfunction.

Keywords

Heart failure; Metabolism; Hexosamine biosynthetic pathway; Glycosylation

Introduction

Heart failure is a leading cause of death in the United States. Because hypertension contributes to cardiac hypertrophy and is a prominent risk factor for developing heart failure, it is important to understand its molecular regulation. In addition to the structural changes that occur during cardiomyocyte hypertrophy, numerous metabolic changes are engaged, which may favor accessory pathways of glucose metabolism, namely, the hexosamine biosynthetic pathway (HBP). The HBP culminates in the production of the high-energy sugar donor uridine diphosphate *N*-acetylglucosamine (UDP-GlcNAc). UDP-GlcNAc serves as a substrate for O-GlcNAc transferase (OGT), the enzyme that catalyzes the O-linkage of β-*N*-acetylglucosamine (O-GlcNAc) to serine and threonine residues on proteins. O-GlcNAcylation serves as posttranslational signaling mechanism that becomes elevated during times of cellular stress [18, 19, 41, 42], such as myocardial infarction (MI) [38] or pressure overload [6].

Recently, our lab and others have demonstrated the importance of O-GlcNAc signaling in the developing [39], hypertrophic [6], and failing heart [38]. Constitutive ablation of cardiomyocyte *Ogt* decreases viability of offspring and produces severe ventricular dysfunction in those that do survive [39]. These hearts exhibit maladaptive remodeling and necrosis [39]. OGT ablation alone in adults is less remarkable, with a gradual decline in cardiac function over a period of months [39]. In the context of heart failure, cardiomyocyte $Ogt^{-/-}$ exacerbates post-infarct-induced cardiac dysfunction in a matter of weeks; cardiomyocyte $Ogt^{-/-}$ hearts demonstrate increased fibrosis and cardiomyocyte death [38]. Clearly, O-GlcNAcylation plays an important role in development and responding to pathological stimuli.

Some of the most robust adaptive cardiac processes occur during pressure overload. The heart responds to increased after load by increasing myocyte size, remodeling the extra-cellular matrix to accommodate growth, and re-initiating the fetal gene program. Previously, we demonstrated that protein O-GlcNAcylation is augmented during pressure overload and O-GlcNAc signaling appears to play an important role in cardiomyocyte hypertrophy through NFAT activation in vitro [6]. Here, we sought to test the hypothesis that *Ogt* plays an indispensable role during pressure overload because of an insufficient hypertrophic response. We used an inducible, cardiomyocyte-specific $Ogt^{-/-}$ mouse to assess the role of *Ogt* in the heart's response to pressure overload.

Methods

All deidentified human samples were obtained with informed consent and in accord with the institutional review board of the University of Louisville. All human heart failure samples were collected from males, age 50–58 years; were classified NYHA IIIb–IV; had elevated BNP levels; and had ejection fractions below 25%. Of the four total patient samples, the etiology of heart failure for one patient was ischemic cardiomyopathy and the other three was determined to be dilated cardiomyopathy. Control samples were purchased from Integrated Laboratory Services—Biotech (ILSbio; Chestertown, MD, USA). All animals were used in compliance with the Guide for the Care and Use of Laboratory Animals issued by the National Institutes of Health. The experimental protocols in this study have been reviewed and approved by the University of Louisville Institutional Animal Care and Use Committee.

Generation of inducible, cardiac-specific *Ogt*-deficient mice

To generate a cardiac *Ogt* KO model, homozygous *Ogt*-floxed mice (originally developed by Dr. Jamey Marth [22]) were crossed with αMHC-driven mutated estrogen receptor flanked cre recombinase (MCM) [32] mice to generate an inducible cardiomyocyte-specific model of *Ogt* ablation as previously described [38, 39]. Inducible, cardiomyocyte-specific *Ogt*-deficient (i-cm$Ogt^{-/-}$) mice and their wild-type littermates were genotyped using previously established protocols [38]. At 12 weeks of age, both i-cm$Ogt^{-/-}$ and WT (*Ogt*-floxed/MCM negative) mice were subjected to tamoxifen treatment and then transverse aortic constriction.

Tamoxifen treatment

Tamoxifen treatment was performed as previously described [38]. To prepare the tamoxifen solution, 4-hydroxytamoxifen (25 mg, Sigma, St. Louis, MO, USA) was added to 1 ml of warmed (37°C) 100% ethanol. The mixture was vortexed and sonicated until fully dissolved. Then, the mixture was added to 9-ml peanut oil (Sigma, St. Louis, MO, USA) and was vortexed and sonicated until dissolved. 4-hydroxytamoxifen (20 mg/kg) was injected intraperitoneally on alternating sides for 5 days. Mice were kept for 5 days following 4-hydroxytamoxifen.

Transverse aortic constriction (TAC) surgery

Three-month-old i-cm$Ogt^{-/-}$ mice and wild-type littermates were subjected to TAC surgery, as described previously [6, 28], following 4-hydroxytamoxifen treatment. At the end of the study, mice were euthanized and the hearts were rapidly excised and weighed. The hearts were then immediately frozen in liquid nitrogen and stored at −80 °C, or, perfused, and fixed for immunohistochemical analysis.

Echocardiography

Transthoracic echocardiography of the left ventricle was performed as previously described [3, 8, 10, 11, 28, 35–38] with adjustments for the Vevo 770 system.

Adult mouse cardiomyocyte (ACM) isolation

Adult mouse cardiomyocytes were isolated from surgically naïve male i-cm*Ogt*$^{-/-}$ mice using the Langendorff perfusion method as previously described [16, 25, 26, 40]. Briefly, mice were injected IP with heparin (3000 units) and anesthetized with 5% isoflurane. Hearts were rapidly excised and washed in ice-cold PBS. The aorta was cannulated with a blunted 23-gauge needle and secured with a 4-0 silk suture. Next, the cannulated heart was attached to the Langendorff apparatus and perfused with oxygenated Tyrode's buffer (18-mmol/l sodium bicarbonate, 126-mmol/l sodium chloride, 4.4-mmol/l potassium chloride, 1-mmol/l magnesium chloride, 4-mmol/l HEPES, 11-mmol/l glucose, 10-mmol/l 2,3-butanedione monoxime, and 30-mmol/l taurine) at 37 °C for 3–5 min. Then, the hearts were perfused with an oxygenated collagenase solution [Tyrode's 0.1% bovine serum albumin (BSA) 0.025-mmol/l calcium chloride 0.1% type II collagenase (Worthington, CLS-2)] for 10–13 min. Following collagenase perfusion, excess fatty tissue, aorta, and atria were carefully removed from the heart and discarded. Next, the left and right ventricles were gently teased apart with fine forceps and triturated with a 10-ml pipette. Myocytes were filtered through a 140-μm nylon mesh filter (NY4H, EMD Millipore, Billerica, MA, USA). Myocytes were allowed to sediment for 15 min. Supernatant was removed and the sedimented myocytes were processed for protein and RNA.

Neonatal rat cardiomyocyte (NRCM) isolation and culture

Neonatal rat cardiomyocytes were isolated from 1–2-day-old Sprague–Dawley rats as previously described [1, 5, 6, 12, 18–21, 29, 30, 33]. NRCMs were plated at a density of 850,000 cells per ml. For the first four days following isolation, NRCMs were cultured in DMEM (D6429, Sigma-Aldrich) containing BrdU (0.1 mM), 5% fetal bovine serum, penicillin (100 U/ml), streptomycin (100 mg/ml), and vitamin B_{12} (2 μg/ml). Following day 4 (post-isolation), BrdU was removed from NRCM medium.

Adenoviral gene transfer

For gene transfer experiments, NRCMs were serum-starved overnight and then transduced with 100 multiplicity of infection (MOI) of replication-deficient adenoviruses carrying OGA gene (Ad-OGA; Vector Biolabs, Malvern, PA, USA), or null virus (Ad-Null; 1240, Vector Biolabs, Malvern, PA, USA) in serum free medium for 5 h as previously described [5, 6, 18–21, 42]. Following virus treatment, NRCMs were returned to complete medium. Protein and RNA were harvested 48-h post-transfection.

Protein isolation

ACM and NRCM cellular protein content was harvested as previously published [38]. Protein was harvested from whole heart tissue as described previously [6, 38].

ACMs, NRCMs, and heart lysate protein concentration were determined by Bradford assay with Bio-Rad protein assay dye reagent (Bio-Rad Laboratories) using different concentrations of bovine serum albumin as standards. Protein concentrations were measured with a Thermo Multiskan Spectrum spectrophotometer.

Immunoblotting

Neonatal rat cardiomyocyte or whole heart protein samples were subjected to electrophoresis in SDS-PAGE gels (4–12%, Invitrogen) and transferred to PVDF membrane (Immobilon-P, EMD Millipore, Billerica, MA, USA) at 4 °C. For O-GlcNAc immunoblotting membranes were allowed to dry at room temperature for 1 h. Then, the blot was probed with primary antibody against: O-GlcNAc: RL2 (1:1000, Affinity Bioreagents) in PBS-casein (Bio-Rad Laboratories) overnight at 4 °C. Membranes were washed three times with 1 × PBS. Membranes were incubated at room temperature with secondary antibody goat anti-mouse IgG-HRP (1:4000, sc-2005; Santa Cruz Biotechnology) in PBS-casein. Membranes were again washed three times with 1x PBS and then imaged. All other western blotting followed standard protocols. Briefly, membranes were blocked at room temperature using Tris-buffered saline pH 7.5 (TBS) containing nonfat milk (5%), washed with TBS containing Tween-20 (TBS-T, 0.1%), and probed with primary antibody. Antibodies for OGT (SQ-17—1:2000, Sigma-Aldrich), OGA (NCOAT—1:1000, Santa Cruz Biotechnology), GATA-4 (14353—1:1000, Cell Signaling Technology), and α-tubulin (T6074—1:2000, Sigma-Aldrich) were made in TBS containing nonfat milk (1%). After overnight incubation at 4 °C, blots were washed in TBS containing Tween-20 (TBS-T, 0.1%). The blots were blocked for 15 min in TBS-T containing 1% milk, washed, and then incubated with goat anti-rabbit IgG-HRP (sc-2004; Santa Cruz Biotechnology or 7074; Cell Signaling Technology) or goat anti-mouse IgG-HRP (Santa Cruz Biotechnology), in 1:2000 dilution (for OGT, OGA, GATA-4, α-smooth muscle actin, and α-tubulin). After washing three times with TBS-T, the membrane was saturated with SuperSignal West Pico Chemiluminescent Substrate (Thermo Fisher Scientific) and imaged on a Fuji LAS-3000 bio-imaging analyzer. To confirm the linear range of the signal, multiple exposures from every experiment were performed. Levels of proteins in each lane were normalized to loading protein content (α-tubulin) or to Ponceau stain and expressed as relative to control (set as 100%).

Enzymatic labeling of O-GlcNAc-modified proteins

O-GlcNAc modified proteins were labeled using Invitrogen's Click-iT enzymatic labeling kit according to the manufacturer's instructions as previously described [20]. In short, azido-modified galactose is transferred onto O-GlcNAc residues and the azido-labeled glycoproteins can be detected with a fluorescent dye, TAMRA. Gels were stained for total protein with Sypro Ruby (to serve as a loading control) gel stain as previously described [20].

Reverse transcriptase PCR and real-time PCR

The total RNA from ACMs, NRCMs, or from hearts was extracted and used to make cDNA as previously described [6, 38, 39]. The relative levels of mRNA transcripts were quantified by real-time PCR using SYBR Green (Thermo Fisher Scientific) on a real-time PCR system (ABI 7900 HT, Applied Biosciences). Most primers were made using NCBI Primer Blast except HPRT primers (PPM03559E-200, QIAGEN) and those referenced (Supplementary Table 1). The data were normalized to mouse HPRT mRNA threshold cycle (C_T) values using the $\Delta\Delta C_T$ comparative method [15]. Primer sequences are listed in Table S1.

Histopathology

Histology was performed using previously published methods [38, 39]. Briefly, formalin-fixed, paraffin embedded hearts from sham and TAC mice were sectioned, deparaffinized, and rehydrated. Masson's trichrome (Richard-Allan Scientific, Masson's trichrome kit, Fisher Scientific, Ottawa, ON, Canada) was used to detect collagen. Cardiac collagen content was determined as the percentage of collagen in long-axis sections of the LV.

To assess cardiomyocyte hypertrophy, cardiac sections were stained with wheat germ agglutinin (WGA; Texas Red-X conjugate, Invitrogen, Carlsbad, CA, USA) to demarcate cell membranes. DAPI was used to detect nuclei. Cardiomyocytes were visualized using a Nikon TE-2000E microscope interfaced with a Nikon A1 confocal system. Cardiomyocyte areas were determined in cardiomyocytes with centrally located nuclei with Nikon Elements software [64bit, version 3.22.00 (Build 710)].

Cardiac apoptosis was assessed by TUNEL positivity. A TUNEL assay kit (TB235, Promega Corporation) was used according to the manufacturer's instructions on LV sections. Sections were also stained with DAPI to identify nuclei. Sections were imaged using a Nikon TiE using a 20× objective. TUNEL positivity was calculated by dividing the total number of TUNEL positive cells by the number of nuclei.

Cardiac capillary density was assessed by isolectin B4 positivity per area (mm^2). Briefly, deparaffinized LV sections were stained with isolectin B4 (DL-1207 DyLight 594, Vector Labs) at dilution of 1:30 for 60 min at 37 °C. Heart sections were stained with DAPI to identify nuclei. Autofluorescence was quenched with Sudan Black (1 mg/ml) staining for 30 min. Sections were imaged with a Nikon TiE with a 20× objective. Capillary density was calculated by dividing the total number of isolectin B4 positive vessels by the area (mm^2).

Statistical analysis

Results are shown as mean ± SD. The statistical analysis (GraphPad 5.0d) was conducted using Student's *t* test or by one-way ANOVA followed by Newman–Keuls multiple comparison test when appropriate. Differences were considered statistically significant if $p < 0.05$.

Results

Protein O-GlcNAcylation is augmented in human heart failure

Due to limited availability of donor hearts, end-stage heart failure patients occasionally receive left ventricular assist devices (LVADs) as a bridge to transplantation. Because we had access to a limited number of patients' myocardial samples, we assessed cardiac O-GlcNAc levels to determine whether O-GlcNAcylation was altered in failing human hearts (Fig. 1a). Specifically, apical cores removed during LVAD implantation were saved; this tissue served as our heart failure (HF) group. Cardiac tissue from severe heart failure patients prior to LVAD implantation (HF) demonstrated augmented protein O-GlcNAcylation when compared with patients without heart disease (control; C) (Fig. 1a, $p < 0.05$). These data combined with our published data [38] are consistent with the notion that

increased O-GlcNAcylation is a pro-adaptive stress response that is a relevant feature in human heart failure.

Cardiomyocyte ablation of *Ogt* decreases protein O-GlcNAcylation following pressure overload

To evaluate the influence of O-GlcNAc on the pro-adaptive response to pressure overload, we used an inducible cardiomyocyte-specific knockout of *Ogt* (i-cm*Ogt*$^{-/-}$). i-cmOgt$^{-/-}$ mice and their wild-type (WT) littermates were subjected to pressure overload (for 2 and 4 weeks). Deletion of *Ogt* diminished OGT mRNA and protein levels ($p < 0.05$) at both 2 weeks (Fig. 1b, c) and 4 weeks (Fig. 1e, f). Accordingly, we observed lower levels of protein O-GlcNAcylation in i-cm*Ogt*$^{-/-}$ when compared with WT at both 2 weeks (Fig. 1d, $p < 0.05$) and 4 weeks (Fig. 1g, $p < 0.05$). As an aside, we determined whether expression of OGA, the enzyme that catalyzes the removal of O-GlcNAc, was altered during pressure overload. OGA mRNA transcript and protein levels were depressed ($p < 0.05$) at 2 weeks in i-cm*Ogt*$^{-/-}$ (Supplemental Figure 1A and B), but not 4 weeks (Supplemental Figure 1C and D).

Cardiomyocyte-specific *Ogt* deletion depresses cardiac function following pressure overload

Cardiac function of i-cm*Ogt*$^{-/-}$ and their WT littermates subjected to transverse aortic constriction (TAC) was assessed via echocardiography at 2 weeks (Fig. 2). Representative M-mode echocardiograms (Fig. 2a) indicated LV dilation in i-cm*Ogt*$^{-/-}$ TAC hearts. Specifically, i-cm*Ogt*$^{-/-}$ mice exhibited significantly increased systolic (Fig. 2b, $p < 0.05$) and diastolic (Fig. 2c, $p < 0.05$) diameters. Fractional shortening was depressed in i-cm*Ogt*$^{-/-}$ compared with wild-type mice (Fig. 2d, $p < 0.05$). In accordance with enlarged ventricular dimensions, i-cm*Ogt*$^{-/-}$ demonstrated a significant decline in ventricular function. Specifically, LV diastolic (Fig. 2e, $p < 0.05$) and systolic (Fig. 2f, $p < 0.05$) volumes were elevated compared with WT; ejection fraction was depressed in i-cm*Ogt*$^{-/-}$ mice (Fig. 2g, $p < 0.05$). Stroke volume (Fig. 2h), heart rate (Fig. 2i), and cardiac output (Fig. 2j) remained unaltered between groups. Ablation of *Ogt* exacerbates cardiac dysfunction following 2 weeks of pressure overload.

Cardiac function of i-cm*Ogt*$^{-/-}$ and WT mice subjected to transverse aortic constriction (TAC) was assessed via echocardiography at 4 weeks (Fig. 3). Representative M-mode echocardiograms (Fig. 3a) indicated ventricular dilation in i-cm*Ogt*$^{-/-}$ compared with WT. The 4-week i-cm*Ogt*$^{-/-}$ group demonstrated increased systolic LV internal diameter (Fig. 3c, $p < 0.05$). Diastolic dimensions were unchanged between groups (Fig. 3b). Because of the systolic defect, fractional shortening was depressed (Fig. 3d, $p < 0.05$) in the i-cm*Ogt*$^{-/-}$ 4 weeks group. Diastolic volume remained unchanged (Fig. 3e), though systolic volume (Fig. 3f, $p < 0.05$) was elevated in i-cm*Ogt*$^{-/-}$ mice; ejection fraction was significantly depressed (Fig. 3g, $p < 0.05$) in i-cm*Ogt*$^{-/-}$ mice. Furthermore, stroke volume decreased (Fig. 3h, $p < 0.05$) in the i-cm*Ogt*$^{-/-}$, while heart rate was increased (Fig. 3i, $p < 0.05$). Cardiac output was significantly depressed in the i-cm*Ogt*$^{-/-}$ cohort (Fig. 3j, $p < 0.05$). The absence of *Ogt* exacerbates ventricular dilation and dysfunction during pressure overload.

Metabolic transcripts are not significantly different without *Ogt* during pressure overload

Heart failure is accompanied by metabolic derangements. To address a potential mechanistic link between *Ogt* ablation and cardiac dysfunction, we assessed the contribution of O-GlcNAc to alterations in metabolic genes involved in fatty oxidation or glycolysis at 2- and 4-week post-TAC (Fig. 4). We observed a reduction in *Pfk1* mRNA, the enzyme responsible for commitment to glycolysis, in the i-cm$Ogt^{-/-}$ group (Fig. 4a, $p < 0.05$) only at 2 weeks, while glucose transporter 1 (*Slc2a1*) and 4 (*Slc2a4*) expression remained unaltered at 2 weeks. Yet, at 4 weeks, we detected a reduction in *Slc2a4* mRNA in the i-cm$Ogt^{-/-}$ TAC group (Fig. 4b, $p < 0.05$). Expression of the gene coding for rate-limiting enzyme in the HBP, *Gfpt2* (Fig. 4a), remained unaltered throughout the 4 weeks time course.

Next, we examined genes involved in fatty acid oxidation. We detected a reduction in *Cpt2* mRNA at 2 weeks the i-cm$Ogt^{-/-}$ TAC group (Fig. 4a, $p < 0.05$), but this did not persist at 4 weeks. Furthermore, PGC1α and PGC1α-dependent genes (*Cpt1b* and *Mcad*) remained unchanged, which could indicate no difference in fatty acid oxidation. We also evaluated potential changes in calcium handling genes (*Serca2a* and *Calm1*), which also remained unchanged. Thus, loss of *Ogt* did not result in a metabolic collapse during TAC.

Ogt is not required for cardiomyocyte hypertrophy during pressure overload

In addition to metabolic alterations, pressure overload induces a hypertrophic gene program. At 2 weeks of TAC, there was no difference in *Nppa* and *Nppb* mRNA (WT TAC vs. i-cm$Ogt^{-/-}$ TAC; Fig. 5a); however, at 4 weeks, *Nppa*, but not *Nppb*, mRNA was significantly higher in the i-cm$Ogt^{-/-}$ TAC hearts compared with WT TAC hearts (Fig. 5b, $p < 0.05$). Despite this difference, cardiomyocyte cross-sectional areas were not significantly different between the i-cm$Ogt^{-/-}$ and WT groups following TAC (Fig. 5c–e). Moreover, according to the heart weight to tibia length ratio, there was no change in LV hypertrophy between WT and KO groups at either time point following TAC (Fig. 5f, g, respectively). Cardiomyocyte *Ogt* appears dispensable in the development of in vivo cardiomyocyte hypertrophy.

Deletion of cardiomyocyte *Ogt* enhances TGFβ2 mRNA following pressure overload

We previously showed that *Ogt* ablation exacerbated post-infarct remodeling, resulting in increased cardiac apoptosis and fibrosis. Here, we demonstrated exacerbated cardiac dysfunction without significant changes in metabolic transcript levels or cardiomyocyte hypertrophy. Thus, we hypothesized that increased fibrosis may partially explain the decline in cardiac function in the i-cm$Ogt^{-/-}$ TAC. We measured mRNA levels of the three isoforms of TGFβ, which is a central regulator of fibrosis. *Tgfb1* and *Tgfb3* mRNA levels were unchanged (Fig. 6a); however, *Tgfb2* mRNA was significantly upregulated at both 2 and 4 weeks of pressure overload in the i-cm$Ogt^{-/-}$ TAC hearts (Fig. 6a, $p < 0.05$).

TGFβ2 is an essential component in cardiac development; hence, only $Tgfb2^{-/-}$ mice result in congenital cardiovascular defects [27]. One of the main functions of TGFβ2 in development is to promote epithelial to mesenchymal transition (EMT). Emerging studies have identified the redeployment of these developmental programs in the adult heart during ischemic injury and cardiac fibrosis [13, 34]. Thus, we hypothesized that enhanced TGFβ2 signaling could promote myocardial fibrosis by inducing fibroblast proliferation and

activation. We measured transcript levels of key mediators of EMT: *Snai1*, *Snai2*, *Twi*, *Zeb1*, and *Zeb2* (Supplemental Figure 2). Interestingly, Snail is a target for O-GlcNAcylation; O-GlcNAcylation of Snail stabilizes it and promotes EMT through transcriptional suppression of E-Cadherin [24]. Here, we observed no difference in EMT signatures at any time point between WT and i-cm*Ogt*$^{-/-}$ (Supplemental Figure 2). There is little evidence for differences in EMT.

In contrast to the role of TGFβ2, basic fibroblast growth factors (FGF2) may be anti-fibrotic [31] in nature and limit myofibroblast differentiation [4, 7]. Here, we observed a reduction in *Fgf2* mRNA at 2 weeks (Fig. 6b). Induction of *Tgfb*2 and concomitant suppression of *Fgf2* could result in enhanced myofibroblast differentiation and fibrosis. To address this question, we measured markers of fibrosis such as *Ctgf*, collagens (1–4) (*Col1a1*, *Col1a2*, *Col3a1*, and *Col4a1*) at the mRNA level, and observed no significant differences (Fig. 6c). At the histological level, there were no differences in fibrosis between the WT and i-cm*Ogt*$^{-/-}$ following 4 weeks TAC (Fig. 6d–f). We conclude that *Ogt* deletion does not exacerbate fibrosis during pressure overload.

Cardiomyocyte-specific *Ogt* deletion suppresses GATA-4 protein expression at 2- and 4-week post-TAC

Transcription factors geared toward lineage commitment and differentiation are redeployed in response to cardiac hypertrophy/injury. We measured transcript levels of adult cardiomyocyte markers (*Myh6* and *Myh7*) and differentiating makers (*Mef2C*, *Nkx2-5*, and *Gata4*) in i-cm*Ogt*$^{-/-}$ and WT groups following 2- and 4-week TAC (Fig. 7a, b). Adult cardiomyocyte gene expression remained unchanged; however, cardiomyocyte deletion of *Ogt* suppressed expression of *Gata4* mRNA (Fig. 7b) and GATA-4 protein (Fig. 7c, d). Because GATA-4 is required for a normal hypertrophic response, the reduction in GATA-4 expression may have contributed to cardiac dysfunction in the i-cm*Ogt*$^{-/-}$ hearts.

To determine whether suppression O-GlcNAcylation was sufficient to reduce expression of GATA-4, we queried whether cardiomyocytes, in the absence of exogenous hypertrophic stimuli, exhibited a similar reduction in *Gata4* mRNA following overexpression of OGA (to decrease O-GlcNAc levels). Indeed, overexpression of OGA in neonatal rat cardiomyocytes reduced *Gata4* mRNA and GATA-4 protein expression (Fig. 7e–h). Next, we wanted to determine whether suppression of GATA-4 expression affected the expression of relevant GATA-4 target genes: *Bcl2* and *Vegfa*. We observed no differences in *Vegfa* mRNA; however, *Bcl2* mRNA expression was significantly increased at 2- and 4-week post-TAC (Supplemental Figure 3A and B). This prompted us to query whether there were differences in apoptosis or angiogenesis between the WT and KO; however, we found no differences in apoptosis (via a TUNEL; Supplementary Figure 3C) or capillary density (via isolectin B4 stain; Supplementary Figure 3D). These data indicate that suppression of O-GlcNAcylation is sufficient to reduce GATA-4 expression, though the mechanisms require further study.

Ogt deletion in cardiomyocytes engages expression of dedifferentiation genes

Although the original hypothesis regarding *Ogt* and in vivo hypertrophy was largely rejected, it remains unclear why the *Ogt*-deficient hearts experienced exacerbated ventricular

dysfunction following pressure overload. To address potential antecedent differences in *Ogt*-deficient cardiomyocytes, we induced recombination in adult mice (with tamoxifen, as described in the Methods) and isolated the resulting *Ogt*-deficient and sufficient (WT) cardiomyocytes (Fig. 8a, b). We assessed markers of remodeling and lineage commitment (Fig. 8c, d). Tgfb1 mRNA was upregulated in i-cm$Ogt^{-/-}$ cardiomyocytes indicating a possible upregulation in TGFB signaling (Fig. 8c). Surprisingly, GATA-4 expression was unchanged in the *Ogt*-deficient cardiomyocytes (Fig. 8d). We also assessed putative markers of dedifferentiation, *Nkx2-5* and *Acta2* (Fig. 8d), and found mRNA levels of both genes were upregulated in i-cm$Ogt^{-/-}$ cardiomyocytes (Fig. 8d). These data indicate that loss of *Ogt* favors *Nkx2-5* and *Acta2* expression, which is consistent with cardiomyocyte dedifferentiation. Although these changes may sensitize cardiomyocytes to subsequent dysfunction during pressure overload, the induction of *Nkx2-5* and *Acta2* are insufficient to induce acute dysfunction in vivo (based on echocardiography data from Sham mice).

Discussion

A number of posttranslational modifications regulate cardiomyocyte hypertrophy and ventricular remodeling during pressure overload. We previously showed that cardiomyocyte *Ogt* plays an essential role in maturation of the heart [39], and loss of cardiomyocyte *Ogt* produces profound derangements in ventricular function following myocardial infarction [38]. Although the induction of O-GlcNAcylation during in vitro cardiomyocyte hypertrophy [6] is essential, it was not clear whether *Ogt* exerts an essential role in regulating hypertrophy during pathophysiologically relevant in vivo models; this was the focus of the present study. Here, we found that O-GlcNAcylation was induced in human heart failure. We also found that deletion of cardiomyocyte *Ogt* exacerbated pressure overload dysfunction without affecting hypertrophy. Because of the decreased expression of the essential cardiac transcription factor GATA-4, we conclude that the exacerbated ventricular function is likely caused by the loss in GATA-4 expression.

Because we previously demonstrated a role for O-GlcNAc in hypertrophic transcriptional reprogramming in vitro [6], we wanted to determine whether such molecular insights might have direct implications in an in vivo model of hypertrophy. Here, we found that patients with severe heart failure (NYHA IIIb–IV) had significantly elevated levels of O-GlcNAcylation. Although these findings do not indicate causality (or prove a pro-adaptive role of O-GlcNAc), they do corroborate our previous findings of increased O-GlcNAcylation in murine heart failure [38]. Our group was the first to demonstrate this concept in a mammalian heart failure system [38]; however, others had subsequently confirmed this general observation in human cardiovascular disease [17]. As more groups develop the capacity to identify the specific proteins modified by O-GlcNAc in disease staged context, it is likely that potential biomarkers and/or therapeutic targets could emerge from this line of inquiry.

The original question that drove this study was whether *Ogt* was necessary for cardiomyocyte hypertrophy in vivo. On face value, the data seem to indicate there was no difference in cardiomyocyte hypertrophy when comparing the WT TAC to the i-cm$Ogt^{-/-}$ TAC; however, there is, perhaps, an additional more nuanced explanation. In general, the i-

cm*Ogt*$^{-/-}$ TAC group exhibited more severe signs of cardiac dysfunction compared with WT. It is possible that O-GlcNAcylation (via *Ogt*) could exert regulatory effects on hypertrophic transcriptional reprogramming, and, given equal extents of disease, a role for *Ogt* on hypertrophy *per se* could be significant; however, if *Ogt* also exerts other effects (not limited to hypertrophy), which offset the balance of disease severity, then discriminating differences in hypertrophy between the WT TAC hearts and i-cm*Ogt*$^{-/-}$ TAC hearts would be confounded. Thus, loss of *Ogt* might exert deleterious effects that exacerbate particular aspects of pathophysiology in the failing heart. Such differences could make the impact of TAC relatively higher in the i-cm*Ogt*$^{-/-}$ hearts. Although speculative, this explanation could potentially reconcile the present in vivo results with our prior in vitro observations [6].

The present data support the conclusion that *Ogt* plays an important pro-adaptive role during cardiac dysfunction. Yet, the precise role of OGT in the hypertrophic/failing heart remains to be fully elucidated. We partially addressed this issue by querying the potential impact of OGT on remodeling, particularly fibrosis. The changes in *Tgfb2* and *Fgf2* expression suggested fibrotic changes, which were not borne out at the histopathologic level. Although the present study focused on the role of cardiomyocyte *Ogt*, it is possible that *Ogt* plays distinct roles in other cell types. We speculate that OGT activity could play an essential role, for example, in fibroblasts.

The reduction in GATA-4 expression was one of the more curious findings in the present study. There is no established relationship between O-GlcNAcylation and GATA-4 expression. It is possible that the reduction in GATA-4 expression is the result of, rather than the cause of, exacerbated ventricular dysfunction. Prior studies showed clearly the role of *Gata4* in the adaptation of the murine heart to pressure overload. Specifically, deletion of cardiomyocyte *Gata4* in adult mice impairs compensatory responses following pressure overload [2, 23]. Thus, it is possible that deletion of cardiomyocyte *Ogt* in the present study partially recapitulated the *Gata4* null phenotype. Future studies could establish whether OGT/OGA activities directly regulate GATA-4 protein expression. It is possible that changes in O-GlcNAcylation could affect the transcription of *Gata4*; however, the reduction in *Gata4* mRNA was underwhelming, and our speculation would favor a posttranscriptional (at least) explanation. In additional experiments, we determined whether decreasing O-GlcNAcylation (via Ad-OGA overexpression) was sufficient to suppress GATA-4 expression. Similar to our observations in the OGT-deficient hearts, we found that OGA overexpression suppressed GATA-4 expression (at mRNA and protein levels). Thus, it seems that a reduction in O-GlcNAcylation (via *Ogt* deletion in vivo or adenoviral overexpression of OGA in vitro) can limit expression of GATA-4.

The more direct question of how loss of cardiomyocyte *Ogt* promotes ventricular dysfunction remains unresolved. To further examine this question, we determined whether differences existed in GATA-4 expression in cardiomyocytes following *Ogt* recombination (without subjecting the mice to TAC). Contrary to the global reduction in GATA-4 in i-cm*Ogt*$^{-/-}$ hearts following TAC, *Gata4* mRNA expression was unchanged in surgically naïve *Ogt*-deficient cardiomyocytes; however, further examination revealed an increase in *Nkx2-5 and Acta2* mRNA expression. Although these changes tempt us to speculate on the role of *Ogt* in cardiomyocyte dedifferentiation, at minimum, the results indicate a shift in the

expression profile of *Ogt*-deficient cardiomyocytes. We hypothesize that such a shift may, in part, explain the sensitivity of *Ogt*-deficient hearts to pressure overload. Nevertheless, based on the present (and previous) cardiac function data, the changes in cardiomyocyte gene expression in *Ogt*-deficient myocytes are apparently insufficient to produce cardiac dysfunction under resting conditions. Future studies may determine whether *Ogt* (or O-GlcNAcylation) is involved in cardiomyocyte dedifferentiation, and whether the antecedent increase in *Acta2* expression underlies the decrement in function following pressure overload.

In summary, *Ogt* is not absolutely essential for the development of cardiomyocyte hypertrophy during pressure overload. Loss of cardiomyocyte *Ogt* exacerbates ventricular dysfunction following pathologic pressure overload without affecting fibrosis. The most salient mechanistic insight was the reduction in GATA-4, whose expression is essential following pressure overload, in the i-cm*Ogt*$^{-/-}$ TAC hearts. Although cardiomyocyte *Ogt* is required for GATA-4 expression during pressure overload, cardiomyocyte reprogramming may occur in the absence of *Ogt*, which sensitizes the heart to pressure overload. Despite these intriguing possibilities, the present data cast doubt on O-GlcNA-cylation (via OGT) as a primary arbiter of cardiomyocyte hypertrophy in vivo.

Supplementary Material

Refer to Web version on PubMed Central for supplementary material.

Acknowledgments

The authors thank Linda Harrison for her expert technical assistance with neonatal cardiomyocyte isolations. In addition, we would like to thank Ms. Jessica Lan-shin Liu, Ms. Yun Shi Long, and Dr. Lakshmanan Annamalai, for their technical assistance with histology.

Funding Dr. Jones has been supported by Grants from the NIH (R01 HL083320, R01 HL094419, P20 RR103492, and P01 HL078825). Mr. Dassanayaka has been supported by an American Heart Association Predoctoral Fellowship—Great Rivers Affiliate (14PRE19710015).

Abbreviations

HBP	Hexosamine biosynthetic pathway
O-GlcNAc	β-O-Linked *N*-acetylglucosamine
OGT	O-GlcNAc transferase
OGA	O-GlcNAcase
TAC	Transverse aortic constriction
PFK1	Phosphofructokinase-1
GFPT1	Glutamine fructose-6-phosphate transaminase 1
GFPT2	Glutamine fructose-6-phosphate transaminase 2
PGC1α	Peroxisome proliferator-activated receptor gamma, co-activator 1 alpha

PGC1β	Peroxisome proliferator-activated receptor gamma, co-activator 1 beta
CPT1b	Carnitine palmitoyltransferase 1b
CPT2	Carnitine palmitoyltransferase 2
MCAD	Medium-chain acyl-CoA dehydrogenase;
PPARα	Peroxisome proliferator-activated receptor alpha
SLC2A1	Solute carrier family 2 (facilitated glucose transporter), member 1
SLC2A4	Solute carrier family 2 (facilitated glucose transporter), member 4
SERCA 2a	Sarco/endoplasmic reticulum Ca^{2+}-ATPase
CALM1	Calmodulin 1
ANP	Atrial natriuretic peptide
BNP	Brain natriuretic peptide
TGFβ1	Transforming growth factor 1
TGFβ2	Transforming growth factor 2
TGFβ3	Transforming growth factor 1
FGF2	Fibroblast growth factor 2
CTGF	Connective tissue growth factor
COL1α1	Collagen, type I, alpha 1
COL1α2	Collagen, type I, alpha 2
COL3α1	Collagen, type 3, alpha 1
COL4α1	Collagen, type 4, alpha 1
MMP2	Matrix metallopeptidase 2
TIMP2	Metallopeptidase inhibitor 2
ZEB1	Zinc finger E-box-binding homeobox 1
ZEB2	Zinc finger E-box-binding homeobox 2
SNAI1	Snail family zinc finger1
SNAI2	Snail family zinc finger1
TWI	Twist basic helix-loop-helix transcription factor 1
VIM	Vimentin
FN1	Fibronectin 1

POSTN	Periostin
MYH6	Alpha myosin heavy chain
MHY7	Beta myosin heavy chain
NKX 2-5	NK2 homeobox 5
MEF2C	Myocyte enhancer factor 2C
GATA4	GATA-binding protein 4
ACTA2	Actin, alpha 2, smooth muscle
BCL2	B-cell lymphoma 2
VEGFA	Vascular endothelial growth factor A

References

1. Akao M, Ohler A, O'Rourke B, Marban E. Mitochondrial ATP-sensitive potassium channels inhibit apoptosis induced by oxidative stress in cardiac cells. Circ Res. 2001; 88:1267–1275. DOI: 10.1161/hh1201.092094 [PubMed: 11420303]
2. Bisping E, Ikeda S, Kong SW, Tarnavski O, Bodyak N, McMullen JR, Rajagopal S, Son JK, Ma Q, Springer Z, Kang PM, Izumo S, Pu WT. Gata4 is required for maintenance of postnatal cardiac function and protection from pressure overload-induced heart failure. Proc Natl Acad Sci USA. 2006; 103:14471–14476. DOI: 10.1073/pnas.0602543103 [PubMed: 16983087]
3. Condorelli G, Roncarati R, Ross J Jr, Pisani A, Stassi G, Todaro M, Trocha S, Drusco A, Gu Y, Russo MA, Frati G, Jones SP, Lefer DJ, Napoli C, Croce CM. Heart-targeted overexpression of caspase3 in mice increases infarct size and depresses cardiac function. Proc Natl Acad Sci USA. 2001; 98:9977–9982. DOI: 10.1073/pnas.161120198 [PubMed: 11493678]
4. Cushing MC, Mariner PD, Liao JT, Sims EA, Anseth KS. Fibroblast growth factor represses Smad-mediated myofibroblast activation in aortic valvular interstitial cells. FASEB J. 2008; 22:1769–1777. DOI: 10.1096/fj.07-087627 [PubMed: 18218921]
5. Dassanayaka S, Readnower RD, Salabei JK, Long BW, Aird AL, Zheng YT, Muthusamy S, Facundo HT, Hill BG, Jones SP. High glucose induces mitochondrial dysfunction independently of protein O-GlcNAcylation. Biochem J. 2015; 467:115–126. DOI: 10.1042/BJ20141018 [PubMed: 25627821]
6. Facundo HT, Brainard RE, Watson LJ, Ngoh GA, Hamid T, Prabhu SD, Jones SP. O-GlcNAc signaling is essential for NFAT-mediated transcriptional reprogramming during cardiomyocyte hypertrophy. Am J Physiol Heart Circ Physiol. 2012; 302:H2122–H2130. DOI: 10.1152/ajpheart.00775.2011 [PubMed: 22408028]
7. Fedak PW, Bai L, Turnbull J, Ngu J, Narine K, Duff HJ. Cell therapy limits myofibroblast differentiation and structural cardiac remodeling: basic fibroblast growth factor-mediated paracrine mechanism. Circ Heart Fail. 2012; 5:349–356. DOI: 10.1161/CIRCHEARTFAILURE.111.965889 [PubMed: 22508775]
8. Greer JJ, Kakkar AK, Elrod JW, Watson LJ, Jones SP, Lefer DJ. Low-dose simvastatin improves survival and ventricular function via eNOS in congestive heart failure. Am J Physiol Heart Circ Physiol. 2006; 291:H2743–H2751. DOI: 10.1152/ajpheart.00347.2006 [PubMed: 16844920]
9. Hakuno D, Kimura N, Yoshioka M, Mukai M, Kimura T, Okada Y, Yozu R, Shukunami C, Hiraki Y, Kudo A, Ogawa S, Fukuda K. Periostin advances atherosclerotic and rheumatic cardiac valve degeneration by inducing angiogenesis and MMP production in humans and rodents. J Clin Invest. 2010; 120:2292–2306. DOI: 10.1172/JCI40973 [PubMed: 20551517]

10. Jones SP, Greer JJ, van Haperen R, Duncker DJ, de Crom R, Lefer DJ. Endothelial nitric oxide synthase overexpression attenuates congestive heart failure in mice. Proc Natl Acad Sci USA. 2003; 100:4891–4896. DOI: 10.1073/pnas.0837428100 [PubMed: 12676984]
11. Jones SP, Greer JJ, Ware PD, Yang J, Walsh K, Lefer DJ. Deficiency of iNOS does not attenuate severe congestive heart failure in mice. Am J Physiol Heart Circ Physiol. 2005; 288:H365–H370. DOI: 10.1152/ajpheart.00245.2004 [PubMed: 15319210]
12. Jones SP, Zachara NE, Ngoh GA, Hill BG, Teshima Y, Bhatnagar A, Hart GW, Marban E. Cardioprotection by *N*-acetyl-glucosamine linkage to cellular proteins. Circulation. 2008; 117:1172–1182. DOI: 10.1161/CIRCULATIONAHA.107.730515 [PubMed: 18285568]
13. Kovacic JC, Mercader N, Torres M, Boehm M, Fuster V. Epithelial-to-mesenchymal and endothelial-to-mesenchymal transition: from cardiovascular development to disease. Circulation. 2012; 125:1795–1808. DOI: 10.1161/CIRCULATIONAHA.111.040352 [PubMed: 22492947]
14. Li M, Krishnaveni MS, Li C, Zhou B, Xing Y, Banfalvi A, Li A, Lombardi V, Akbari O, Borok Z, Minoo P. Epithelium-specific deletion of TGF-beta receptor type II protects mice from bleomycin-induced pulmonary fibrosis. J Clin Invest. 2011; 121:277–287. DOI: 10.1172/JCI42090 [PubMed: 21135509]
15. Livak KJ, Schmittgen TD. Analysis of relative gene expression data using real-time quantitative PCR and the 2(−Delta Delta C(T)) Method. Methods. 2001; 25:402–408. DOI: 10.1006/meth.2001.1262 [PubMed: 11846609]
16. Louch WE, Sheehan KA, Wolska BM. Methods in cardiomyocyte isolation, culture, and gene transfer. J Mol Cell Cardiol. 2011; 51:288–298. DOI: 10.1016/j.yjmcc.2011.06.012 [PubMed: 21723873]
17. Lunde IG, Aronsen JM, Kvaloy H, Qvigstad E, Sjaastad I, Tonnessen T, Christensen G, Gronning-Wang LM, Carlson CR. Cardiac O-GlcNAc signaling is increased in hypertrophy and heart failure. Physiol Genomics. 2012; 44:162–172. DOI: 10.1152/physiolgenomics.00016.2011 [PubMed: 22128088]
18. Ngoh GA, Facundo HT, Hamid T, Dillmann W, Zachara NE, Jones SP. Unique hexosaminidase reduces metabolic survival signal and sensitizes cardiac myocytes to hypoxia/reoxygenation injury. Circ Res. 2009; 104:41–49. DOI: 10.1161/CIRCRESAHA.108.189431 [PubMed: 19023128]
19. Ngoh GA, Hamid T, Prabhu SD, Jones SP. O-GlcNAc signaling attenuates ER stress-induced cardiomyocyte death. Am J Physiol Heart Circ Physiol. 2009; 297:H1711–H1719. DOI: 10.1152/ajpheart.00553.2009 [PubMed: 19734355]
20. Ngoh GA, Watson LJ, Facundo HT, Dillmann W, Jones SP. Non-canonical glycosyltransferase modulates post-hypoxic cardiac myocyte death and mitochondrial permeability transition. J Mol Cell Cardiol. 2008; 45:313–325. DOI: 10.1016/j.yjmcc.2008.04.009 [PubMed: 18539296]
21. Ngoh GA, Watson LJ, Facundo HT, Jones SP. Augmented O-GlcNAc signaling attenuates oxidative stress and calcium overload in cardiomyocytes. Amino Acids. 2011; 40:895–911. DOI: 10.1007/s00726-010-0728-7 [PubMed: 20798965]
22. O'Donnell N, Zachara NE, Hart GW, Marth JD. Ogt-dependent X-chromosome-linked protein glycosylation is a requisite modification in somatic cell function and embryo viability. Mol Cell Biol. 2004; 24:1680–1690. [PubMed: 14749383]
23. Oka T, Maillet M, Watt AJ, Schwartz RJ, Aronow BJ, Duncan SA, Molkentin JD. Cardiac-specific deletion of Gata4 reveals its requirement for hypertrophy, compensation, and myocyte viability. Circ Res. 2006; 98:837–845. DOI: 10.1161/01.RES.0000215985.18538.c4 [PubMed: 16514068]
24. Park SY, Kim HS, Kim NH, Ji S, Cha SY, Kang JG, Ota I, Shimada K, Konishi N, Nam HW, Hong SW, Yang WH, Roth J, Yook JI, Cho JW. Snail1 is stabilized by O-GlcNAc modification in hyperglycaemic condition. EMBO J. 2010; 29:3787–3796. DOI: 10.1038/emboj.2010.254 [PubMed: 20959806]
25. Powell T, Twist VW. A rapid technique for the isolation and purification of adult cardiac muscle cells having respiratory control and a tolerance to calcium. Biochem Biophys Res Commun. 1976; 72:327–333. [PubMed: 985476]
26. Readnower RD, Brainard RE, Hill BG, Jones SP. Standardized bioenergetic profiling of adult mouse cardiomyocytes. Physiol Genomics. 2012; 44:1208–1213. DOI: 10.1152/physiolgenomics.00129.2012 [PubMed: 23092951]

27. Sanford LP, Ormsby I, Gittenberger-de Groot AC, Sariola H, Friedman R, Boivin GP, Cardell EL, Doetschman T. TGFbeta2 knockout mice have multiple developmental defects that are non-overlapping with other TGFbeta knockout phenotypes. Development. 1997; 124:2659–2670. [PubMed: 9217007]

28. Sansbury BE, DeMartino AM, Xie Z, Brooks AC, Brainard RE, Watson LJ, DeFilippis AP, Cummins TD, Harbeson MA, Brittian KR, Prabhu SD, Bhatnagar A, Jones SP, Hill BG. Metabolomic analysis of pressure-overloaded and infarcted mouse hearts. Circ Heart Fail. 2014; 7:634–642. DOI: 10.1161/CIRCHEARTFAILURE.114.001151 [PubMed: 24762972]

29. Sansbury BE, Jones SP, Riggs DW, Darley-Usmar VM, Hill BG. Bioenergetic function in cardiovascular cells: the importance of the reserve capacity and its biological regulation. Chem Biol Interact. 2011; 191:288–295. DOI: 10.1016/j.cbi.2010.12.002 [PubMed: 21147079]

30. Sansbury BE, Riggs DW, Brainard RE, Salabei JK, Jones SP, Hill BG. Responses of hypertrophied myocytes to reactive species: implications for glycolysis and electrophile metabolism. Biochem J. 2011; 435:519–528. DOI: 10.1042/BJ20101390 [PubMed: 21275902]

31. Santiago JJ, McNaughton LJ, Koleini N, Ma X, Bestvater B, Nickel BE, Fandrich RR, Wigle JT, Freed DH, Arora RC, Kardami E. High molecular weight fibroblast growth factor-2 in the human heart is a potential target for prevention of cardiac remodeling. PLoS One. 2014; 9:e97281.doi: 10.1371/journal.pone.0097281 [PubMed: 24827991]

32. Sohal DS, Nghiem M, Crackower MA, Witt SA, Kimball TR, Tymitz KM, Penninger JM, Molkentin JD. Temporally regulated and tissue-specific gene manipulations in the adult and embryonic heart using a tamoxifen-inducible Cre protein. Circ Res. 2001; 89:20–25. [PubMed: 11440973]

33. Teshima Y, Akao M, Jones SP, Marban E. Uncoupling protein-2 overexpression inhibits mitochondrial death pathway in cardiomyocytes. Circ Res. 2003; 93:192–200. DOI: 10.1161/01.RES.0000085581.60197.4D [PubMed: 12855674]

34. von Gise A, Pu WT. Endocardial and epicardial epithelial to mesenchymal transitions in heart development and disease. Circ Res. 2012; 110:1628–1645. DOI: 10.1161/CIRCRESAHA.111.259960 [PubMed: 22679138]

35. Wang J, Wang Q, Watson LJ, Jones SP, Epstein PN. Cardiac overexpression of 8-oxoguanine DNA glycosylase 1 protects mitochondrial DNA and reduces cardiac fibrosis following transaortic constriction. Am J Physiol Heart Circ Physiol. 2011; 301:H2073–H2080. DOI: 10.1152/ajpheart.00157.2011 [PubMed: 21873502]

36. Wang J, Xu J, Wang Q, Brainard RE, Watson LJ, Jones SP, Epstein PN. Reduced cardiac fructose 2,6 bisphosphate increases hypertrophy and decreases glycolysis following aortic constriction. PLoS One. 2013; 8:e53951.doi: 10.1371/journal.pone.0053951 [PubMed: 23308291]

37. Wang Q, Donthi RV, Wang J, Lange AJ, Watson LJ, Jones SP, Epstein PN. Cardiac phosphatase-deficient 6-phospho-fructo-2-kinase/fructose-2,6-bisphosphatase increases glycolysis, hypertrophy, and myocyte resistance to hypoxia. Am J Physiol Heart Circ Physiol. 2008; 294:H2889–H2897. DOI: 10.1152/ajpheart.91501.2007 [PubMed: 18456722]

38. Watson LJ, Facundo HT, Ngoh GA, Ameen M, Brainard RE, Lemma KM, Long BW, Prabhu SD, Xuan YT, Jones SP. O-linked beta-*N*-acetylglucosamine transferase is indispensable in the failing heart. Proc Natl Acad Sci USA. 2010; 107:17797–17802. DOI: 10.1073/pnas.1001907107 [PubMed: 20876116]

39. Watson LJ, Long BW, DeMartino AM, Brittian KR, Readnower RD, Brainard RE, Cummins TD, Annamalai L, Hill BG, Jones SP. Cardiomyocyte Ogt is essential for postnatal viability. Am J Physiol Heart Circ Physiol. 2014; 306:H142–H153. DOI: 10.1152/ajpheart.00438.2013 [PubMed: 24186210]

40. Wolska BM, Solaro RJ. Method for isolation of adult mouse cardiac myocytes for studies of contraction and microfluorimetry. Am J Physiol. 1996; 271:H1250–H1255. [PubMed: 8853365]

41. Zachara NE, O'Donnell N, Cheung WD, Mercer JJ, Marth JD, Hart GW. Dynamic O-GlcNAc modification of nucleocytoplasmic proteins in response to stress. A survival response of mammalian cells. J Biol Chem. 2004; 279:30133–30142. DOI: 10.1074/jbc.M403773200 [PubMed: 15138254]

42. Zafir A, Readnower R, Long BW, McCracken J, Aird A, Alvarez A, Cummins TD, Li Q, Hill BG, Bhatnagar A, Prabhu SD, Bolli R, Jones SP. Protein O-GlcNAcylation is a novel cytoprotective

signal in cardiac stem cells. Stem Cells. 2013; 31:765–775. DOI: 10.1002/stem.1325 [PubMed: 23335157]

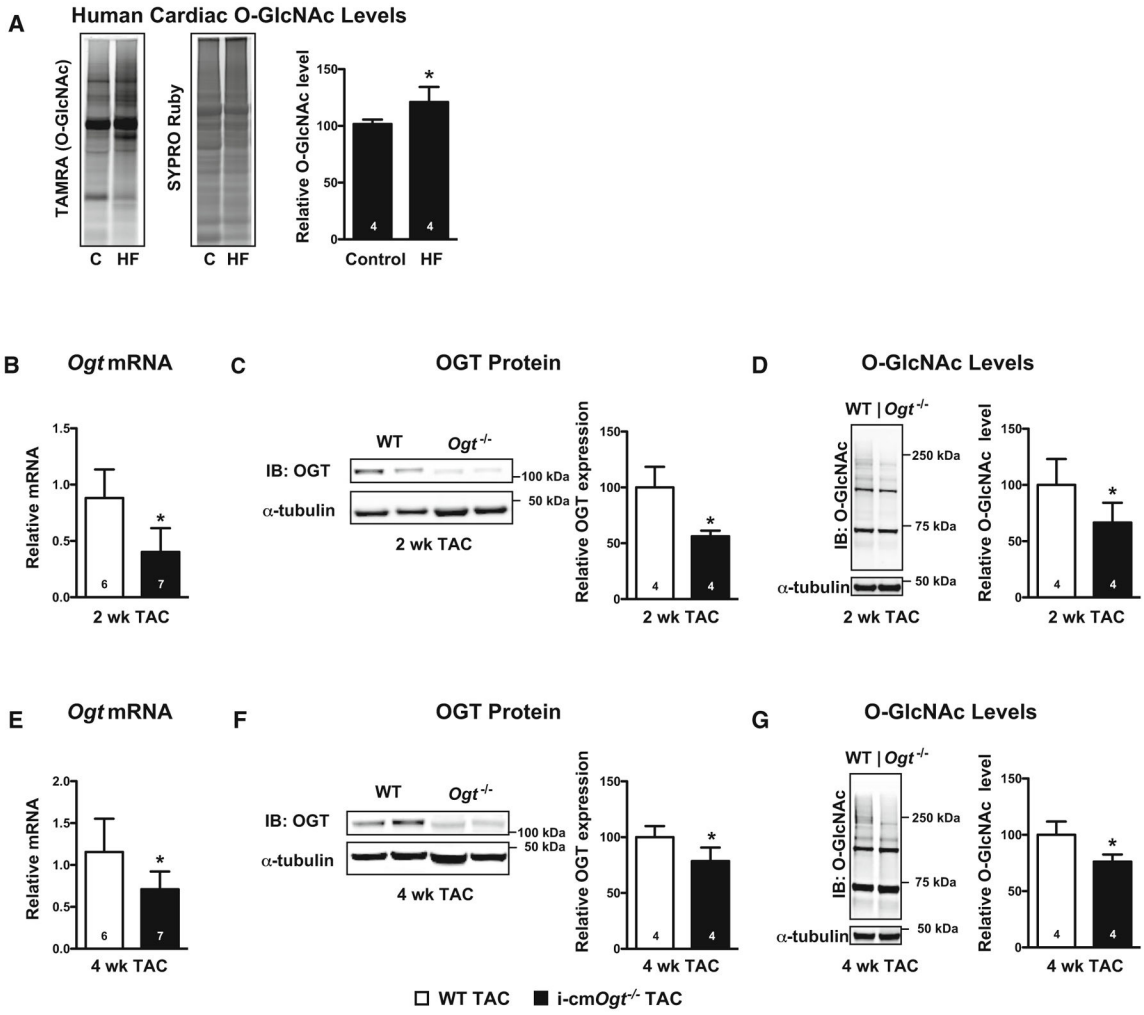

Fig. 1.

Ogt ablation depresses protein O-GlcNAcylation following pressure overload. Human O-GlcNAcylation (**a**) was measured from cardiac biopsies of disease free patients (control; C) and heart failure (HF) patients. TAMRA-positive bands indicate the presence of O-GlcNAc. SYPRO Ruby stain was used to indicate total protein content and served as a loading control. Cardiac OGT mRNA and protein levels were measured following TAC in mice with cardiac-specific deletion of *Ogt*. *Ogt* mRNA, OGT protein, and O-GlcNAc levels were depressed in i-cm$Ogt^{-/-}$ mice at both 2 weeks (**b**–**d**) and 4 weeks (**e**–**g**) following pressure overload. *$p < 0.05$ vs. WT TAC (or vs. control human heart group, as in **a**)

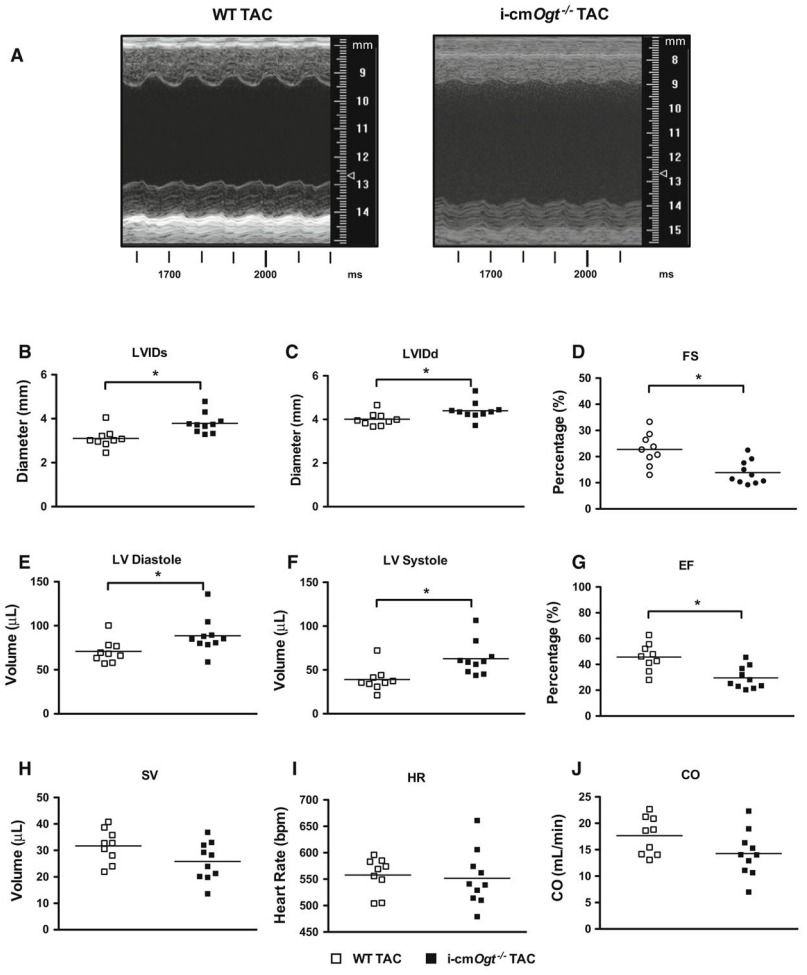

Fig. 2.

Ogt ablation depresses cardiac function following 2 weeks of pressure overload. OGT ablation depresses cardiac function. Following cardiac-specific ablation of *Ogt*, mice were subjected to pressure overload. Echocardiography was taken at 2 weeks with representative M modes of WT and i-cm$Ogt^{-/-}$ TAC (**a**). Cardiac ablation of *Ogt* prior to TAC demonstrated significant increases in diastolic (**b**) and systolic (**c**) diameters and depressed fractional shortening (**d**) at 2 weeks. Cardiac left ventricular diastolic (**e**) and systolic (**f**) volumes were also increased with a concomitant reduction in ejection fraction (**g**). Stroke volume (**h**), heart rate (**i**), and cardiac output (**j**) were not disturbed after 2 weeks of pressure overload. *$p < 0.05$ vs. WT TAC

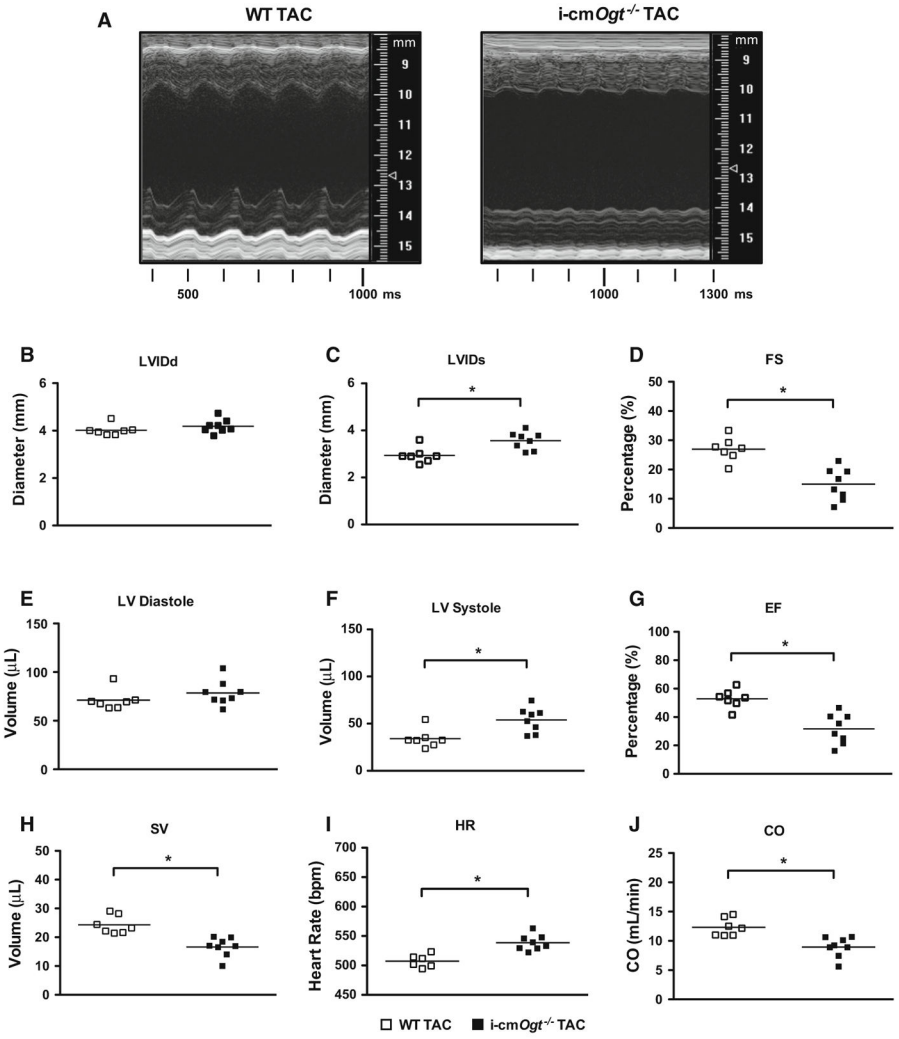

Fig. 3.

Ogt ablation exacerbates cardiac dysfunction following 4 weeks of pressure overload. *Ogt* ablation exacerbates pressure overload-induced heart failure. Cardiac function was assessed with echocardiography after 4 weeks of TAC. Representative M modes for WT and i-cm$Ogt^{-/-}$ are shown (**a**). At 4 weeks, diastolic diameter was not changed (**b**), but systolic diameter (**c**) was increased in i-cm$Ogt^{-/-}$. *Ogt* ablation exacerbated fractional shortening (**d**). Left ventricular diastolic volume (**e**) was unaltered; however, systolic volume (**f**) was significantly increased. Ejection fraction worsened in i-cm$Ogt^{-/-}$ mice (**g**). Stroke volume was depressed (**h**), heart rate increased (**i**), and cardiac output (**j**) was exacerbated in i-cm$Ogt^{-/-}$ after 4 weeks of TAC. *$p < 0.05$ vs. WT TAC

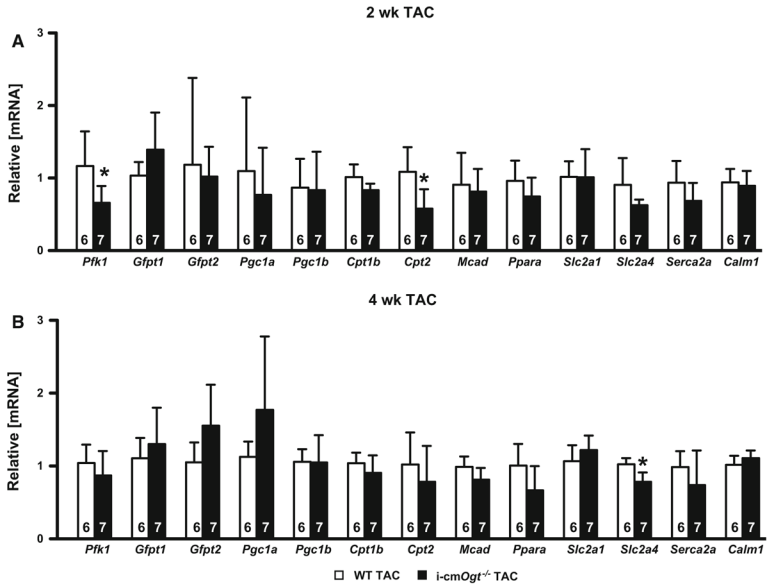

Fig. 4.

Metabolic transcripts are not significantly different without *Ogt* during pressure overload. Cardiac mRNA metabolic profiles of WT TAC and i-cm$Ogt^{-/-}$ TAC were analyzed at 2 (**a**) and 4 weeks (**b**). *Ogt* ablation in cardiomyocytes demonstrated decreased *Pfk1* and *Cpt2* expression 2-week post-TAC, indicating alterations in glycolytic and fatty acid metabolism, respectively. Furthermore, *Slc2a4* mRNA was depressed in O-GlcNAc-attenuated cohort indicating a reduction in insulin-mediated glucose cell entry. *$p < 0.05$ vs. WT TAC

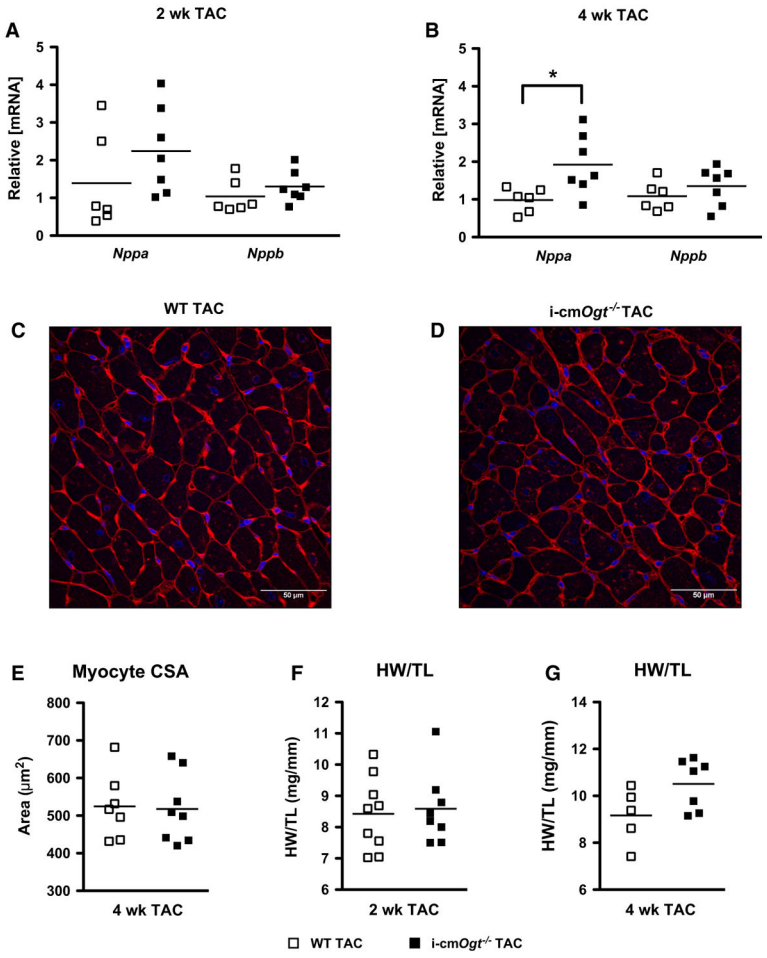

Fig. 5.

Ogt is not required for cardiomyocyte hypertrophy during pressure overload. Mediators of cardiac hypertrophy, *Nppa* and *Nppb,* were measured following 2 and 4 weeks of pressure overload (**a**, **b**). *Ogt* deletion did not alter *Nppa* and *Nppb* expression at 2 weeks. *Nppa* expression increased at 4-week post-TAC (**b**). Hearts from 4 weeks WT TAC (**c**) and i-cm$Ogt^{-/-}$ TAC (**d**) were stained with wheat germ agglutinin and DAPI. Myocyte cross-sectional area (CSA; **e**) remained unchanged between WT TAC and i-cm$Ogt^{-/-}$ TAC. Heart weight to tibia length ratio was measured at 2 (**f**) and 4 (**g**)-week post-TAC. *$p < 0.05$ vs. WT TAC

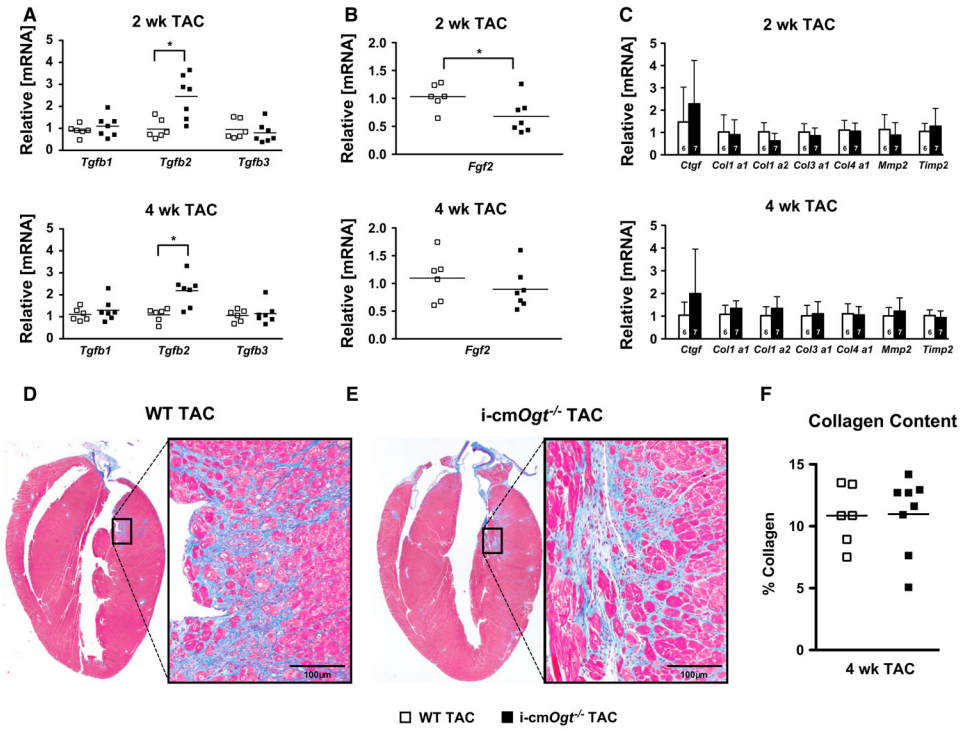

Fig. 6.

Cardiac-specific deletion of *Ogt* enhances TGFβ2 mRNA at 2 and 4 weeks following pressure overload. Markers of cardiac fibrosis were assessed via RT-PCR in WT and i-cm$Ogt^{-/-}$ cohorts following 2 and 4 weeks of TAC. Gene expression of TGFβ, major regulator of cardiac fibrosis, demonstrated significant upregulation of *Tgfb2* isoform at both 2 and 4 weeks (**a**). Coincidentally, a known repressor of TGFβ1 mediated signaling, FGF2, demonstrated depressed mRNA expression at 2 weeks. We subsequently measured collagen mRNA expression at 2- and 4-week post-TAC (**b**). *Col1a1, Col1a2, Col3a1*, and *Col4a2* mRNA expression remained unaltered between groups (**c**). Following 4 weeks of pressure overload, whole hearts from WT TAC (**d**) and i-cm$Ogt^{-/-}$ TAC (**e**) mice were excised, sectioned, and stained with Masson's trichrome to measure cardiac fibrosis. i-cm$Ogt^{-/-}$ TAC hearts exhibited no difference in cardiac collagen content from WT TAC hearts. *$p < 0.05$ vs. WT TAC. *$p < 0.05$ vs. WT TAC

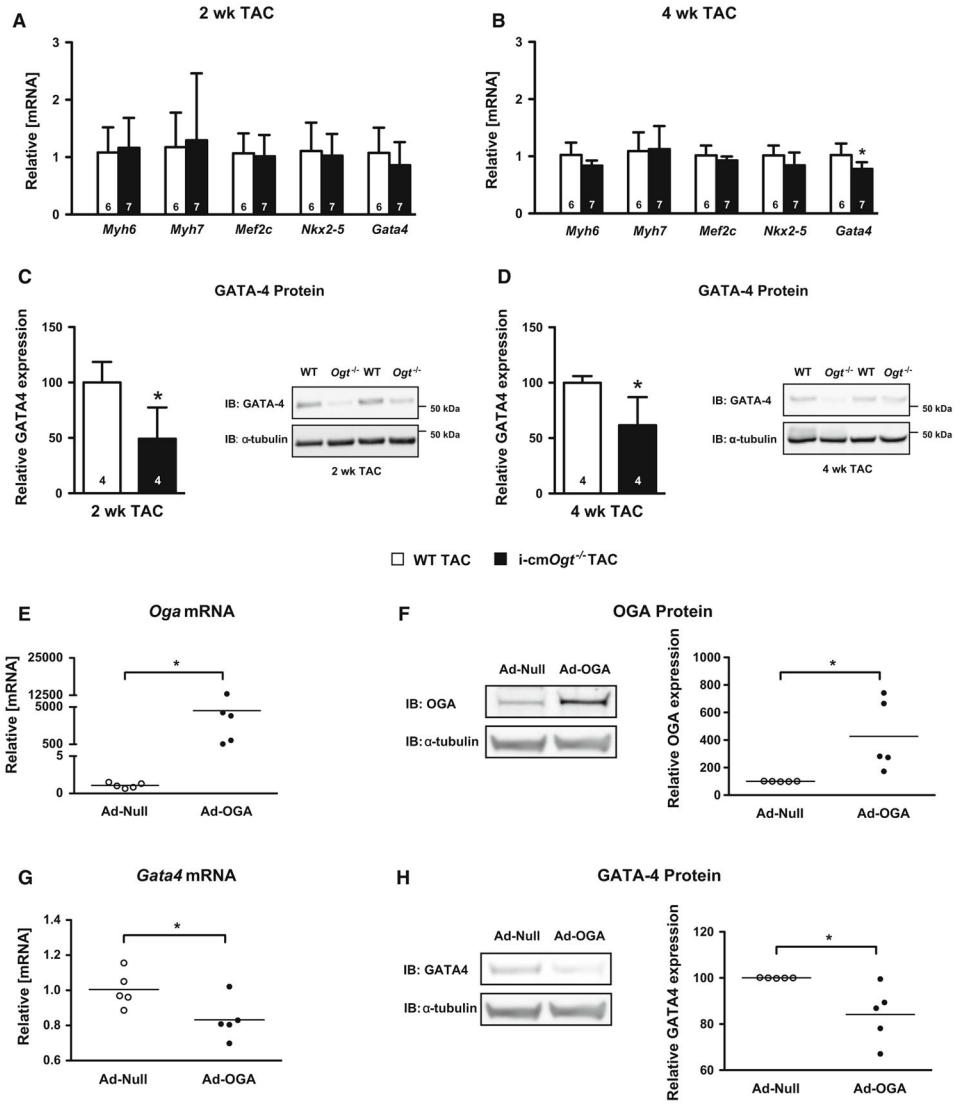

Fig. 7.

Cardiomyocyte deletion of *Ogt* suppresses GATA-4 expression during pressure overload. Markers of differentiation and lineage were detected via RT-PCR in WT and i-cm$Ogt^{-/-}$ groups following 2 and 4 weeks of TAC. Gene expression of adult cardiomyocyte markers (*Myh6, Myh7*) remained unchanged (**a**, **b**) in both 2- and 4-week TAC groups. Markers of lineage commitment (*Mef2c, Nxk2-5, and Gata4*) remained unchanged at 2-week post-TAC (**a**). At 4-week post-TAC, *Gata4* mRNA expression was significantly down-regulated in the i-cm$Ogt^{-/-}$ group (**b**). GATA-4 protein expression was assessed at both 2 and 4 weeks (**c**, **d**). GATA-4 protein was significantly depressed at both 2 and 4 weeks in the i-cm$Ogt^{-/-}$ groups. In additional experiments, NRCMs were transduced with adenovirus to overexpress OGA (which decreases O-GlcNAc levels). OGA overexpression was verified by qRT-PCR (**e**) and western blotting (**f**). In these same NRCMs, *Gata4* mRNA (**g**) and GATA-4 protein expression (**h**) were measured. *$p < 0.05$ vs. WT TAC

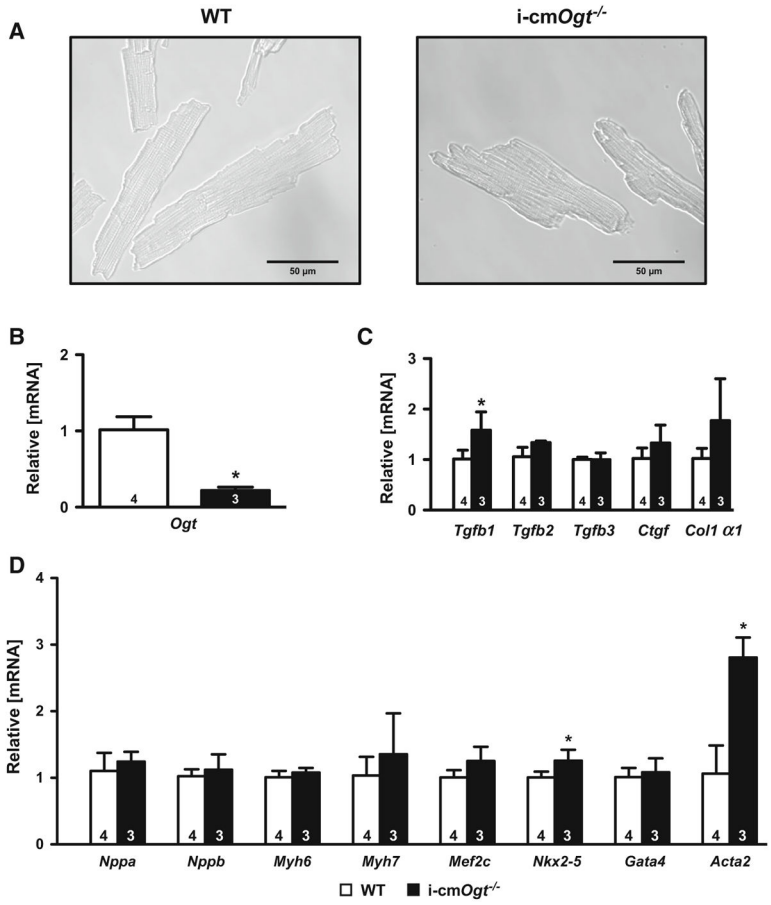

Fig. 8.

Ogt deletion in surgically naïve cardiomyocytes enhances genes indicative of dedifferentiation. Cardiomyocytes were isolated from surgically naïve WT and i-cm$Ogt^{-/-}$ mice 5-day post-tamoxifen treatment (**a**). *Ogt* mRNA suppression was verified in i-cm$Ogt^{-/-}$ cardiomyocytes (**b**). Markers of fibrosis were largely unchanged except for an increase in *Tgfb1* mRNA in i-cm$Ogt^{-/-}$ cardiomyocytes (**c**). Markers of remodeling and lineage commitment were assessed in WT and i-cm$Ogt^{-/-}$ cardiomyocytes (**d**). *Nkx2-5* and *Acata2* mRNA were upregulated in i-cm$Ogt^{-/-}$ cardiomyocytes (**d**). *$p < 0.05$ vs. WT